

Nanoscale

Accepted Manuscript



This is an *Accepted Manuscript*, which has been through the Royal Society of Chemistry peer review process and has been accepted for publication.

Accepted Manuscripts are published online shortly after acceptance, before technical editing, formatting and proof reading. Using this free service, authors can make their results available to the community, in citable form, before we publish the edited article. We will replace this *Accepted Manuscript* with the edited and formatted *Advance Article* as soon as it is available.

You can find more information about *Accepted Manuscripts* in the [Information for Authors](#).

Please note that technical editing may introduce minor changes to the text and/or graphics, which may alter content. The journal's standard [Terms & Conditions](#) and the [Ethical guidelines](#) still apply. In no event shall the Royal Society of Chemistry be held responsible for any errors or omissions in this *Accepted Manuscript* or any consequences arising from the use of any information it contains.

COMMUNICATION

Pressure Sensor Based on the Orientational Dependence of Plasmonic Properties of Gold Nanorods

Cite this: DOI: 10.1039/x0xx00000x

Lishun Fu,^{ab} Yiding Liu,^{bc} Wenshou Wang,^{ab} Mingsheng Wang,^b Yaocai Bai,^{bc} Eric L. Chronister,^b Liang Zhen^{*a} and Yadong Yin^{*bc}

Received 00th January 2012,
Accepted 00th January 2012

DOI: 10.1039/x0xx00000x

www.rsc.org/

A novel pressure sensor has been developed by taking advantage of the orientational dependence of localized surface plasmon resonance of gold nanorods embedded in a polymer matrix. This stress-responsive material can be used to record distribution and magnitude of pressure between two contacting surfaces by outputting optical response.

Plasmonic metal nanostructures have received considerable attention due to their broad applications in optoelectronics,¹⁻³ sensing,⁴⁻⁶ catalysis⁷⁻⁹ and photothermal therapy.¹⁰⁻¹² In particular, Au or Ag nanorods (NRs) have been the focus of research in many fields because they display two modes of localized surface plasmon resonance (LSPR) in extinction spectra: transverse and longitudinal modes, compared to a single excitation mode for spherical particles.^{13, 14} The origin of these two LSPR modes is the difference in excitation from the perpendicular and parallel components of the electric field of incident light relative to the main axis of the rod.¹⁵ As the longitudinal excitation is highly sensitive to the length,^{16, 17} the plasmonic property of such nanorods can be tuned in a wide spectrum range by controlling their aspect ratio, which can now be conveniently achieved through colloidal synthesis.

Theoretically, due to the shape anisotropy of noble metal nanorods, the two LSPR modes can be selectively excited by controlling their relative orientation to incident light. For example, when AuNRs are oriented perpendicular to the incident light, both transverse and longitudinal modes could be excited, resulting in two LSPR bands in the extinction spectrum. When they are parallel to the incident angle, only the transverse mode can be excited. As a result, only the resonance band for the transverse mode displays in the corresponding extinction spectrum while the absorption band for the longitudinal mode is inhibited. Figure 1a shows the simulated extinction spectra of a AuNR with its orientation varying from parallel to perpendicular to the direction of incident light, obtained using the discrete dipole approximation (DDA, see details in the supporting information).^{18, 19} It can be clearly seen that the intensity of the longitudinal mode of the AuNR decreases monotonically when the angle between the gold nanorod and incident light changes from 90 to 0°. The angular dependence of the intensity of the two resonance modes can be revealed more clearly by plotting the ratio of the intensity of longitudinal to transverse modes against the

relative angle between the AuNR and the incident light. As shown in Figure 1b, the intensity ratio increases monotonically with the increasing angle. Thus, it is expected that plasmonic tuning can be achieved by controlling the orientation of AuNRs. In our previous work, we have revealed selective excitation of the two LSPR modes of AuNRs can be achieved by controlling their orientation via external magnetic fields.²⁰

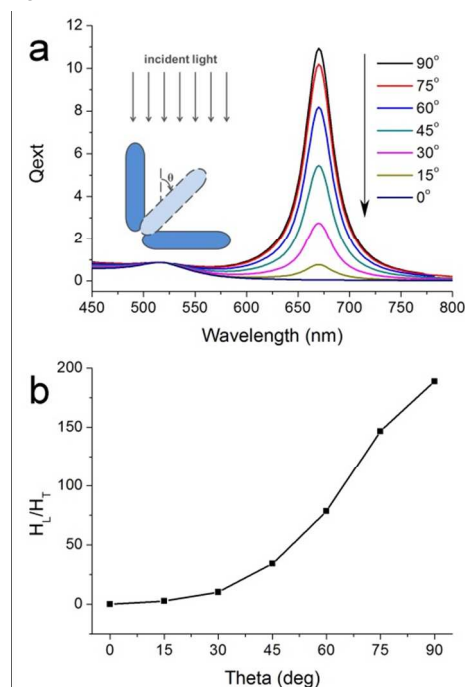


Figure 1. (a) DDA simulations of extinction efficiency spectra of one AuNR (cylinder with hemispherical end-caps, length: 42nm, diameter: 16nm, 7584 dipoles were used in the calculation) in different orientations under unpolarized incident light. (b) The intensity ratio of longitudinal and transverse modes of one AuNR in different orientations based on DDA simulations.

In this work, we report a new pressure sensor that can be used to monitor applied pressure based on the orientational dependence of LSPR of AuNRs upon the incidence of ordinary light. Figure 2a illustrates our design principle. The pressure sensor is composed of a

composite film in which AuNRs are homogeneously embedded in a polymer matrix.²¹ Initially, AuNRs are randomly oriented.¹⁵ When the composite film is subjected to an external pressure, polymer flow is induced in the plane perpendicular to the force direction and AuNRs are expected to rotate in this flow field. The realignment of the AuNRs to a more ordered state causes changes in the relative intensity of the two LSPR absorption bands.^{22, 23} A pressure sensor can thus be established by correlating the applied pressure with the change in the optical property of the composite film.

To understand the realignment behavior of embedded AuNRs in the polymer matrix when subjected to an external pressure, we here qualitatively describe the rotation of AuNRs from mechanical force analysis. When the composite film is subjected to an external force F which is perpendicular to the film plain, a radial flow of the polymer will be induced. For the sake of simplicity of analysis, we only consider the planar deformation of the composite film and assume that the total volume remains unchanged during polymer deformation. As shown in the cross sectional view in Figure 2b, a simple planar extensional flow is expected in the polymer matrix. The vertical component of the flow velocity is supposed to decrease with the increase of the depth of the film, while the horizontal component of the flow velocity is supposed to increase with the increase in the distance from the central point of the force. The suspended nanorods under this velocity gradient are expected to show rotational and translational movements. Since the orientation-dependent plasmonic property of AuNRs is only sensitive to the relative angle between the long axis of nanorod and the incident direction of the light (which is typically normal to the film surface), here we can simply consider the orientation change of AuNRs relative to the direction of z axis.

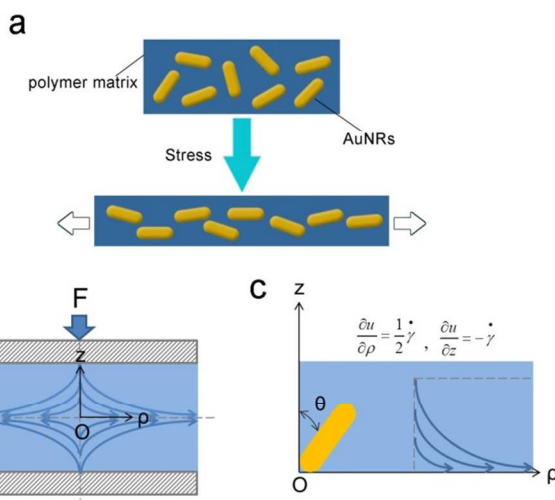


Figure 2. (a) Schematic illustration of the design of the stress-responsive film based on direction related change of LSPR of AuNRs. (b) Velocity distribution of the polymer during deformation. (c) Coordinate system used for the analysis of the direction change of a single particle with aspect ratio r in a simple planar extensional flow.

The rotational motion for rigid cylindrical particles in an extensional flow can be described by Jeffery equations.²⁴ In a simple planar extensional flow ($\frac{\partial u}{\partial \rho} = \dot{\gamma}/2$, $\frac{\partial u}{\partial z} = -\dot{\gamma}$, where u is the fluid velocity, $\dot{\gamma}$ is the deformation rate in the thickness direction which

changes with time), as shown in Figure 2c, the angle in the ρz plane (which corresponds to the cross section shown in Fig 2b) of a single particle with aspect ratio r is given in the equation (the derivation details are shown in the supporting information):

$$\tan \theta = \tan \theta_0 \cdot \exp\left(\frac{3}{2} \frac{r_e^2 - 1}{r_e^2 + 1} \gamma\right) \quad (1)$$

where θ is the azimuthal angle at time t , θ_0 is the azimuthal angle at initial stage (0 s), r_e is the 'equivalent ellipsoidal' axis ratio of the particle ($r_e = 1.14r^{0.844}$),²⁵ γ is the cumulative deformation ($\gamma = \int \dot{\gamma} dt$).

So after the deformation of the polymer, the orientation of AuNRs changes from its original random state to a new state which is more inclined towards the direction perpendicular to the external force. Thus, it is expected that the intensity ratio of the two resonance modes of AuNRs ($I_{\text{long}}/I_{\text{trans}}$) should increase after experiencing external forces, and in principle such change can be used to indicate the pressure that the system has experienced.

To fabricate the composite film, we first synthesized AuNRs using a slightly modified version of the seed-mediated growth method reported by El-Sayed *et al.*¹³ Then the AuNRs were dispersed in the mixed solution of polyvinyl alcohol (PVA) and polyethylene glycol (PEG) to form a viscous suspension, which was finally casted on a substrate to produce a composite film after evaporation of the solvent. PVA was chosen due to its excellent solubility in water, low optical absorption in visible range, relatively strong adhesion to Au surface, and good film forming property by solution casting.¹⁵ PEG (typically PEG-400), which is fully mixable with PVA, is known as a good plasticizer that can improve the fluidity of the composite film.²¹

Compared with AuNRs solution, the AuNR-polymer films show slight red shift in the resonance peak (Figure S2) due to the increase in refractive index of the surrounding medium (1.333 for water, 1.519 for PVA, 1.467 for PEG). No peak broadening was observed in the spectra, indicating that AuNRs were well-dispersed in the composite polymer without much aggregation.^{15, 22} The thickness of AuNR-polymer film was about 400 μm , as estimated from the cross section of the film by an optical microscope (Figure S3). The gold concentration per composite film area was estimated to be 0.15 - 0.20 mg/cm^2 . The volume fraction of AuNRs was much smaller than the square of aspect ratio $1/r^2$, thus qualifying our system as a dilute suspension in which nanorods can freely rotate.²⁶ Indeed, the calculated average interparticle spacing of AuNRs is much greater than their own dimension so that AuNRs are free to move and rotate, making it possible to use the film deformation for pressure sensing.

In order to perform compression test, AuNR-polymer composite films were first cut into small circular pieces with a diameter of 3 mm using a homemade puncher. These pieces of films have the same initial area as the compression area of sapphire anvil cell (SAC). The samples were then loaded into the anvil cell and constant forces were applied by adding weight onto the homemade device used for *in-situ* real-time UV-vis measurement, as shown in Figure S4. The pressure applied on the sample was calculated by dividing the force by the compression area of SAC.

To evaluate the performance of the composite films, we first applied a constant pressure (2×10^3 psi) to one AuNR-polymer film for a period of 5 min. It was obvious that the intensity of both transverse and longitudinal excitations of AuNRs decreased during compression, as indicated in Figure 3a. This can be ascribed to the decrease in the area concentration of AuNRs due to the expansion of the area of composite film and the decrease in thickness upon the application of pressure. On the other hand, the peak position of two

modes of LSPR did not change during compression, indicating no obvious change in the shape of AuNRs. However, the change in the relative intensity of the two resonance bands was not as dramatic as expected from the simulation. This is mainly because the extinction spectra obtained by the DDA simulation are for one AuNR with a defined orientation, while the actual composite film is composed of many AuNRs with various orientations and aspect ratios. Also in reality the film expansion is often not substantial so that the orientational change of AuNRs in the polymer flow is limited.

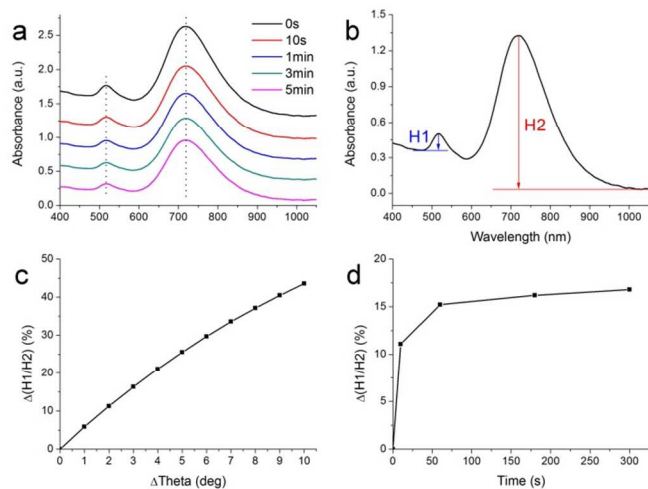


Figure 3. (a) The absorbance spectra of AuNRs in polymer after experiencing a fixed pressure for different time. For the sake of clarity, the curves are arbitrarily shifted along the y-axis. (b) Definition of the intensity of transverse and longitudinal mode of LSPR of AuNRs. (c) Plot of $\Delta(H1/H2)$ for one AuNR changing orientation derived from the DDA simulation results. The angle between the AuNR and incident light is initially set as 45° and increases in the step of 1° . (d) Plot of $\Delta(H1/H2)$ for film experiencing a fixed pressure for different time derived from the absorbance spectra in (a).

Quantitative analysis of the changes of transverse and longitudinal modes requires defining a proper baseline for the resonance bands. For the sake of simplicity, we choose left shoulder of the band as the baseline of the transverse mode while right shoulder as the baseline of the longitudinal mode, as schematically shown in Figure 3b. The intensity of the transverse and longitudinal modes of LSPR was denoted as H1 and H2, respectively. It is noted that the baseline for the transverse absorption peak is much higher than that for the longitudinal absorption peak. This is because there exists non-LSPR absorption from 5d electron transition in the extinction profile before 496 nm and this portion of extinction should not be included in an LSPR absorption peak.²⁷

As discussed before, the ratio between these two modes of surface plasmon resonance H1/H2 is related only to the AuNR direction. To clearly correlate the small changes in relative intensity of the resonance bands to the orientational change of the nanorods, we define $\Delta(H1/H2)$ as follows

$$\Delta(H1/H2) = \frac{(H1/H2)_0 - (H1/H2)_t}{(H1/H2)_0} \quad (2)$$

where $(H1/H2)_0$ and $(H1/H2)_t$ are the intensity ratios between two modes at initial stage (0 s) and time t , respectively. We first confirmed the significant dependence of $\Delta(H1/H2)$ on the orientation of the nanorods using the simulated data. As shown in Figure 3c, if we set the initial angle of a AuNR relative to the incident light at 45° , and allow it to rotate for just a few degrees, the ratio between the two modes of LSPR changes significantly. For example, when the angle between the AuNR and the incident light increases for 3° ,

$\Delta(H1/H2)$ can reach 16.32 %, demonstrating the suitability of using this value for studying the plasmonic changes associated with the small variation in the orientation of AuNRs. Its effectiveness is also confirmed by treating the extinction spectra of the composite film after experiencing the pressure for different period of time (Figure 3a). The corresponding $\Delta(H1/H2)$ values, as shown in Figure 3d, vary more obviously than the extinction spectra themselves.

As indicated in Equation 1, the change of azimuthal angle of AuNRs is expected to increase with an increase in the cumulative deformation. Burgers model composed of Maxwell spring, Maxwell dashpot, and Kelvin unit is widely used to analyze the viscoelasticity of materials, and can give the strain response under constant stress. The cumulative deformation γ at time t can be expressed as:²⁸

$$\gamma = \frac{\sigma_0}{E_M} + \frac{\sigma_0}{E_K} (1 - e^{-t/\tau}) + \frac{\sigma_0}{\eta_M} t \quad (3)$$

where σ_0 is the initially applied stress; E_M and η_M are the modulus and viscosity of the Maxwell spring and dashpot, respectively; E_K and η_K are the modulus and viscosity of the Kelvin spring and dashpot, respectively; $\tau = \eta_K/E_K$ is the retardation time taken to produce $(1 - e^{-1})$ of the total deformation in the Kelvin unit. The first term is constant and can describe the instantaneous elastic deformation; the second term is delayed elasticity of the Kelvin unit and dominant in the earliest stage of creep, but soon goes to a saturation value close to σ_0/E_K ; the third term describes the viscous flow which then increases nearly linearly after a sufficient long period of loading. So the creep of polymer is divided into three stages: the first is the instantaneous elastic stage; the second is the transition stage of creep in which the deformation rate decreases; and the third is the steady stage of creep in which the deformation rate changes very little. The Equations 1 and 3 suggest that the azimuthal angle of AuNRs with a fixed aspect ratio in the radial profile of composite film is expected to increase with an increase in the intensity and duration of applied stress. Accordingly, the ratio between the transverse and longitudinal excitation modes will decrease, leading to a change of $\Delta(H1/H2)$. To verify this assumption, we applied different pressures (4×10^3 , 3×10^3 , 2×10^3 and 1×10^3 psi) to a batch of composite films for the same period of time. During pressing, the changes of extinction spectra for a series of application time (10 s, 1 min, 3 min and 5 min) were recorded. Figure 4a plots the dependence of $\Delta(H1/H2)$ on the pressure applied on the film for a series of application time. When keeping the applied pressure constant, we found that $\Delta(H1/H2)$ increased very quickly in the first 10 s, then the increase slowed down, and remained almost unchanged after 1 min. Using the relationship of $\Delta(H1/H2)$ and orientation change shown in Figure 3c, we can obtain the orientation change of AuNRs in films with time, as shown in Figure S5. It is found that the angle between the AuNR and incident light increased very quickly first, which corresponds to instantaneous elastic deformation; then the angular velocity slowed down eventually, which corresponds to the transition stage of creep; finally the angle between the AuNR and incident light remained almost unchanged, which corresponds to the steady stage of creep. When we fixed the duration of applied stress at 3 min, $\Delta(H1/H2)$ at pressure 1×10^3 , 2×10^3 , 3×10^3 and 4×10^3 psi is 6.73 %, 16.25 %, 22.88 % and 27.40 %, respectively, as shown in Figure 4b. As expected, the composite films show larger directional changes under higher pressures. These experimental results are consistent well with our theoretical considerations. The polymer flow-induced directional change of AuNRs can be utilized for constructing pressure sensors that can reflect the mechanical stress experienced by the composite film, as long as the relation between $\Delta(H1/H2)$ and the applied stress at a series of fixed duration can be pre-established for a particular type of composite film.

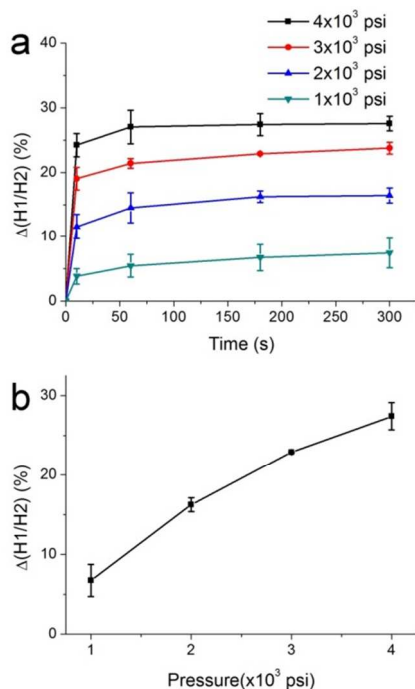


Figure 4. (a) Plots of $\Delta(H1/H2)$ for films experiencing different pressures for a series of application time. (b) Plot of $\Delta(H1/H2)$ for films that experienced different pressures for 3 min.

As demonstrated in Equation 1, AuNRs with larger aspect ratio tend to incline more in the direction perpendicular to the applied stress. To verify this assumption, we applied a fixed pressure (4×10^3 psi) to composite films containing AuNRs with different aspect ratios for the same period of time. Figure 5a shows the dependence of $\Delta(H1/H2)$ on the aspect ratio of AuNRs. While the film containing AuNRs with aspect ratio 2.06 reached a ratio change of 24.15 %, the increase of aspect ratio of AuNRs led to a larger response to the same external pressure, with $\Delta(H1/H2)$ rising to 27.40 % for the case of aspect ratio 2.31 and 35.26 % for the case of aspect ratio 2.60. This result is consistent with the theoretical consideration: when the AuNRs are more inclined in the direction perpendicular to the applied pressure, the ratio change of the two LSPR modes increases more.

The Equations 1 and 3 also suggest that $\Delta(H1/H2)$ is related to the viscoelasticity of polymer if the applied stress is fixed. To extend the pressure response range and also adjust the sensitivity of the AuNR-polymer composite film, we can adjust the fluidity of polymer by controlling the ratio between PVA and PEG. With increased loading of PEG in the polymer, the deformation of the composite film became more sensitive to the applied pressure, as reflected in the change of extinction spectra of the AuNR-polymer composite film. By keeping the pressure (4×10^3 psi) and the application time (3 min) fixed, we examined the $\Delta(H1/H2)$ of the composite film containing AuNRs with a fixed aspect ratio of 2.31. As shown in Figure 5b, while the sample containing 20 wt% PEG only reached a small $\Delta(H1/H2)$ (9.98 %), the increase of the concentration of PEG led to more significant response to the external pressure with $\Delta(H1/H2)$ rising to 14.49 %, 20.91 %, 27.40 %, 33.57 % for the cases with 30 wt%, 40 wt%, 50 wt%, 60 wt% of PEG. These results clearly show that the orientational change of AuNRs in the polymer film is more significant in a more flexible film which contains a larger amount of PEG. Therefore, by changing the amount of plasticizer, it becomes possible to produce polymer films with different pressure sensitivity for a wide range of pressure detection.

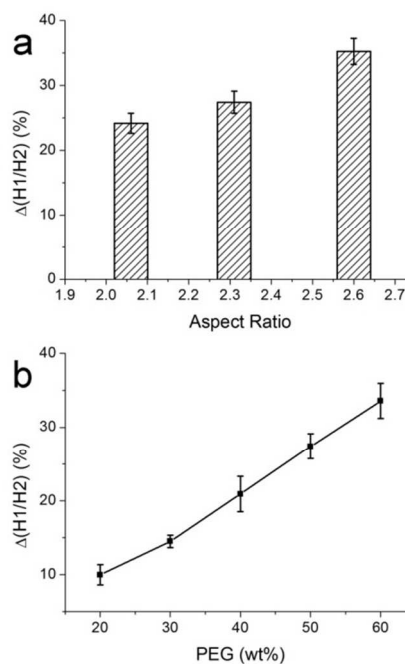


Figure 5. (a) Plot of $\Delta(H1/H2)$ for films containing AuNRs with different aspect ratios that experienced 4×10^3 psi for 3 min. (b) Plot of $\Delta(H1/H2)$ for films doped with different amounts of PEG being treated with 4×10^3 psi for 3 min.

In summary, we have developed a pressure-responsive film based on the orientational dependence of the LSPR of AuNRs. Driven by the deformation of the surrounding polymer matrix under pressure, AuNRs change their orientation and subsequently the intensity ratio of transverse and longitudinal modes of LSPR. While the magnitude of change in the intensity ratio of the two resonance modes depends on the intensity and duration of applied pressure, it can also be controlled by the aspect ratio of the AuNRs and the fluidity of the polymer matrix. Compared with conventional mechanical/electronic pressure sensors which are considerably bulky and not suitable for applications that involve very small areas or objects with complex surface geometries, this unique pressure indicating film is versatile and can be utilized to record the local distribution and magnitude of pressure between two contacting surfaces with complex topological conditions by outputting optical response. This work also illustrates that the orientational dependence of LSPR of anisotropic plasmonic nanostructures may be employed to design novel stimuli responsive devices. Our future work will include replacing Au with Ag which is cheaper and has much stronger plasmonic response in order to reduce the materials cost. For broader applications, we will also explore the possibilities of enhancing the response rate and enabling reversible sensing by selecting appropriate polymer matrix.

Financial support of this work was provided by U. S. National Science Foundation (CHE-1308587). L.S.F. acknowledges the fellowship support by the China Scholarship Council (CSC).

Notes and references

^a School of Materials Science and Engineering, Harbin Institute of Technology, Harbin 150001, China. Email: lzhen@hit.edu.cn

^b Department of Chemistry, University of California, Riverside, CA 92521, USA. E-mail: yadong.yin@ucr.edu

^c Materials Science and Engineering Program, University of California, Riverside, CA 92521, USA.

Electronic Supplementary Information (ESI) available: Experimental details, TEM images, UV-vis spectra, a photograph of homemade equipment for UV-vis measurement. See DOI: 10.1039/c000000x/

1. M. W. Knight, H. Sobhani, P. Nordlander and N. J. Halas, *Science*, 2011, **332**, 702-704.
2. C. Clavero, *Nat Photon*, 2014, **8**, 95-103.
3. S.-B. Wang, R.-S. Chen, S. J. Chang, H.-C. Han, M.-S. Hu, K.-H. Chen and L.-C. Chen, *Nanoscale*, 2014, **6**, 1264-1270.
4. S. M. Marinakos, S. H. Chen and A. Chilkoti, *Anal. Chem.*, 2007, **79**, 5278-5283.
5. N. R. Jana and T. Pal, *Adv. Mater.*, 2007, **19**, 1761-1765.
6. N. Karker, G. Dharmalingam and M. A. Carpenter, *ACS Nano*, 2014, **8**, 10953-10962.
7. S. H. Yoo and S. Park, *Adv. Mater.*, 2007, **19**, 1612-1615.
8. P. Hu, Y. Song, L. Chen and S. Chen, *Nanoscale*, 2015, **7**, 9627-9636.
9. M. Wen, S. Takakura, K. Fuku, K. Mori and H. Yamashita, *Catalysis Today*, 2015, **242, Part B**, 381-385.
10. B. Jang, Y. S. Kim and Y. Choi, *Small*, 2011, **7**, 265-270.
11. M. L. Brongersma, N. J. Halas and P. Nordlander, *Nat Nano*, 2015, **10**, 25-34.
12. M. M. Mkandawire, M. Lakatos, A. Springer, A. Clemens, D. Appelhans, U. Krause-Buchholz, W. Pompe, G. Rodel and M. Mkandawire, *Nanoscale*, 2015, **7**, 10634-10640.
13. B. Nikoobakht and M. A. El-Sayed, *Chem. Mat.*, 2003, **15**, 1957-1962.
14. N. R. Jana, L. Gearheart and C. J. Murphy, *Chemical Communications*, 2001, 617-618.
15. B. M. I. van der Zande, L. Pages, R. A. M. Hikmet and A. van Blaaderen, *J. Phys. Chem. B*, 1999, **103**, 5761-5767.
16. L. Vigderman, B. P. Khanal and E. R. Zubarev, *Adv. Mater.*, 2012, **24**, 4811-4841.
17. J. A. Edgar, A. M. McDonagh and M. B. Cortie, *Acs Nano*, 2012, **6**, 1116-1125.
18. B. T. Draine and P. J. Flatau, *J. Opt. Soc. Am. A-Opt. Image Sci. Vis.*, 1994, **11**, 1491-1499.
19. N. B. Piller and O. J. F. Martin, *IEEE Trans. Antennas Propag.*, 1998, **46**, 1126-1137.
20. M. S. Wang, C. B. Gao, L. He, Q. P. Lu, J. Z. Zhang, C. Tang, S. Zorba and Y. D. Yin, *J. Am. Chem. Soc.*, 2013, **135**, 15302-15305.
21. X. G. Han, Y. D. Liu and Y. D. Yin, *Nano Lett.*, 2014, **14**, 2466-2470.
22. J. Perez-Juste, B. Rodriguez-Gonzalez, P. Mulvaney and L. M. Liz-Marzan, *Adv. Funct. Mater.*, 2005, **15**, 1065-1071.
23. H. Pletsch, M. Tebbe, M. Dulle, B. Förster, A. Fery, S. Förster, A. Greiner and S. Agarwal, *Polymer*, 2015, **66**, 167-172.
24. G. B. Jeffery, *Proc. R. Soc. London, Ser. A*, 1922, **102**, 161-179.
25. J. Harris and J. Pittman, *Journal of Colloid and Interface Science*, 1975, **50**, 280-282.
26. T. Paphanasiou and D. C. Guell, *Flow-induced alignment in composite materials*, Elsevier, 1997.
27. J. H. Simmons and K. S. Potter, *Optical Materials*, Academic Press, 2000.
28. J. L. Yang, Z. Zhang, A. K. Schlarb and K. Friedrich, *Polymer*, 2006, **47**, 6745-6758.

TOC Graphic:

